10 Particle Physics with LHCb

J. Anderson, R. Bernet, A. Bursche, A. Büchler, N. Chiapolini, M. De Cian, Ch. Elsasser, K. Müller, J. Palacios (until January 11), Ch. Salzmann, S. Saornil, N. Serra, St. Steiner, O. Steinkamp, U. Straumann, J. van Tilburg (until March 11), M. Tobin, A. Vollhardt

The full LHCb collaboration consists of 54 institutes from Brazil, China, France, Germany, Ireland, Italy, The Netherlands, Poland, Romania, Russia, Spain, Switzerland, Ukraine, the United Kingdom and the United States of America.

(LHCb - Collaboration)

The LHCb [1] experiment is the smallest of the four large experiments at the Large Hadron Collider (LHC) and is dedicated to b-physics. The main goal of the experiment is the indirect search for New Physics (NP) through precision measurements of CP violating phases and rare heavy-quark decays. Of particular interest are processes that are strongly suppressed in the Standard Model (SM), such as flavour-changing neutral current $b \to s$ transitions. In these loop mediated processes, NP can lead to significant deviations from SM predictions through additional amplitudes involving new heavy particles. These indirect searches extend the discovery potential for new particles to a mass range far beyond that accessible in direct searches. Moreover, observing the pattern of deviations from SM predictions will give insights into the underlying dynamics of the NP and will permit the parameters of New Physics models to be constrained.

The analysis strategies for six selected key measurements have been described in detail in the LHCb "roadmap" document [2]. They comprise measurements of the CKM angle γ from $B \to DK$ tree decays and from penguin-mediated charmless charged two-body B decays, the measurement of the $B_s^0 \bar{B}_s^0$ mixing phase ϕ_s, the determination of the branching fraction of the very rare decay $B_s^0 \to \mu^+\mu^-$, measurements of angular distributions in the rare decay $B^0 \to K^\star \mu^+ \mu^-$, and measurements of radiative $b \to s\gamma$ decays.

10.1 The LHCb detector

To exploit best the strongly forward peaked $b\bar{b}$ production cross section at the LHC, the LHCb detector is laid out as a single-arm forward spectrometer. Its acceptance covers polar angles from 15 mrad to 300 mrad in the bending plane of the spectrometer magnet and 250 mrad in the non-bending plane. This corresponds to a pseudo-rapidity coverage of about $1.9 < \eta < 4.9$. LHCb captures almost 40% of the $b\bar{b}$ production cross section at the LHC while covering only about 4% of the solid angle. An additional benefit of measuring at small polar angles is the possibility to trigger on low-p_T particles down to transverse momenta p_T of only a few GeV. The detector has been described in previous annual reports [3] and in [1].

10.2 Detector performance and first running experience

The LHCb experiment was fully operational from the first day of LHC collisions at a centre of mass energy of 0.9 TeV end of autumn 2009, except for the computing farm for the higher-level triggers (HLT), which was only partially installed. About 37 pb^{-1} of pp collisions at 7 TeV were collected during the 2010 LHC run, with a data taking efficiency of more than 90%. The polarity of the LHCb spectrometer magnet was reversed several times to minimise possible systematics due to detector asymmetries.

LHC running conditions and the instantaneous

luminosity provided by the accelerator evolved rapidly throughout the 2010 run. As the LHC luminosity increased, trigger conditions were gradually tightened such that the available readout bandwidth and CPU in the HLT farm were fully exploited. Data were taken at the highest luminosity available from LHC at all times, although during the later part of the run this meant operating the experiment at significantly higher numbers of pp interactions per bunch crossing than foreseen under nominal conditions. Peak instantaneous luminosities close to the LHCb nominal luminosity were achieved towards the end of the 2010 run, but with only 344 instead of 2622 colliding bunches. These running conditions corresponded to an average number of visible interactions per bunch crossing, μ, of up to 2.4, where nominal LHCb operating conditions correspond to $\mu = 0.4$. The HLT farm has been completed over the 2010/2011 Christmas break.

The instantaneous luminosity will gradually increase in in 2011 running period and about 1 fb^{-1} are expected to be delivered until the end of 2011. For many of the key physics channels at LHCb, significant measurements can already be expected from the 2010/2011 LHC run. The collaboration has already published three papers [4–6] and presented many new results at conferences [8–28].

An excellent vertex resolution is essential for the high-level trigger and for many physics analyses. To minimise extrapolation errors from the first measurement points to the vertex position, the LHCb vertex detector is installed inside the LHC vacuum vessel. The sensitive area of the detector starts at a distance of only 8 mm from the beam axis during data taking. The detectors have to be retracted by 3 cm during beam injection. An internal alignment of better than 5 μm of the vertex detector has been obtained. Fill-to-fill variations in the position of the detectors are also as small as 5 μm. A single-hit resolution of 4 μm has been measured for the innermost readout strips. The measured track impact parameter resolution is slightly worse than expected from simulation, possible reasons for this are being investigated.

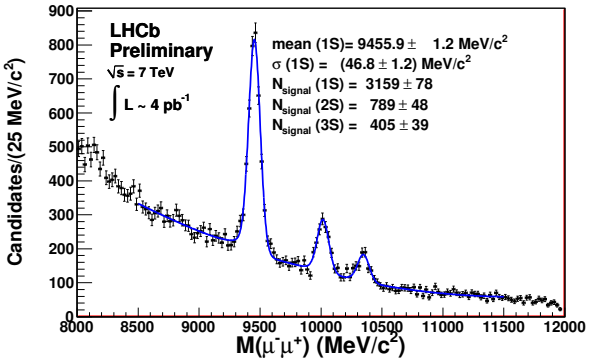

Fig. 10.1 – $\mu^+\mu^-$ invariant mass distribution showing the $\Upsilon(1s)$, $\Upsilon(2s)$ and $\Upsilon(3s)$ resonances.

Good momentum and invariant mass resolutions are crucial for the rejection of combinatorial backgrounds. Measured spatial resolutions in the tracking system are approaching those expected from test beams and simulation. Small differences are remaining from residual misalignments. Since the acceptance of the LHCb tracking system for cosmics is negligibly small, its spatial alignment relies entirely on beam data. The good progress in the understanding of the alignment is demonstrated by the invariant mass resolution obtained for $J/\Psi \to \mu^+\mu^-$ decays, which was 17.1 MeV in May 2010 and had reached 13.3 MeV in December 2010. From simulation, an invariant mass resolution of 12.1 MeV is expected. Figure 10.1 shows a $\mu^+\mu^-$ invariant mass distribution in the mass range of the $\Upsilon(1s)$, $\Upsilon(2s)$ and $\Upsilon(3s)$ resonances. An invariant mass resolution of 47 MeV is obtained, here, and the three resonances are clearly resolved.

An excellent kaon/pion separation over a wide momentum range is another important ingredient for many analyses. Two RICH detectors with three different radiators cover momenta down to about 2 GeV, needed to identify kaons for B flavour tagging, and up to 100 GeV, required for a clean separation of two-body hadronic B decays.

The particle-identification performance has been studied with data using tag-and-probe methods on $\phi \to K^+K^-$, $K^0_s \to \pi^+\pi^-$ and $\Lambda \to p\pi$ decays and is found to be close to expectations from simulation over the full momentum range. The importance of kaon/pion separation for two-body hadronic B decays is illustrated in Fig. 10.2. The

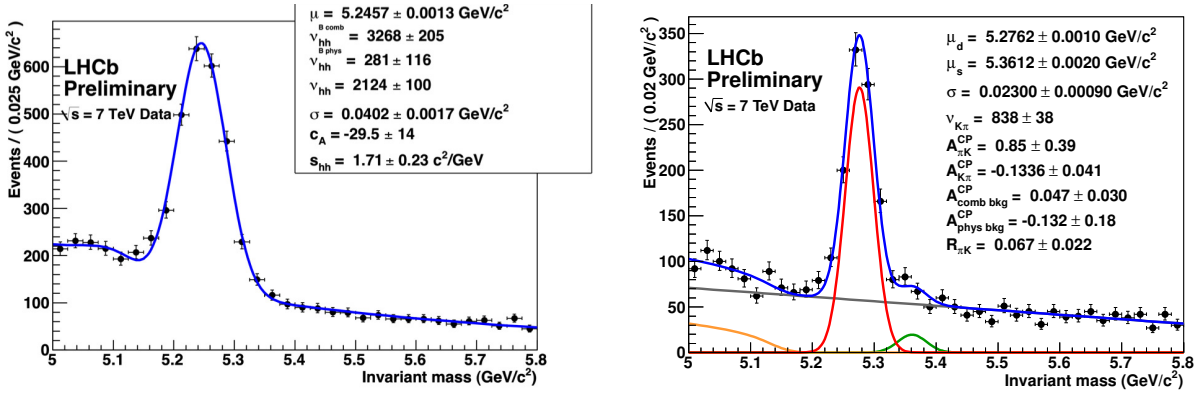

Fig. 10.2 – Left: $B \to h^+h^-$ invariant mass distribution where the pion mass hypothesis was applied for both final-state particles. Right: $B^0_{d,s} \to K^\pm\pi^\mp$ using only loose kaon and pion identification criteria.

left plot shows a $B \to h^+h'^-$ invariant mass spectrum before particle-identification cuts, where the pion mass hypothesis was applied for both final-state particles. Despite the good invariant mass resolution, the contributions from $B^0 \to \pi^+\pi^-$, $B \to K^\pm\pi^\mp$ and $B^0_s \to K^+K^-$ cannot be separated kinematically. The right plot shows the invariant mass spectra for $B^0_s \to K^+K^-$ after particle-identification cuts have been applied. A clean signal with excellent invariant-mass resolution of 23 MeV is observed here as well as for the other two decay modes.

Finally, the performance of the electromagnetic calorimeter in electron and photon reconstruction is illustrated in Fig. 10.3, which shows an e^+e^- invariant mass distribution with a clear $\chi_{c1,2} \to J/\psi\gamma$ signal.

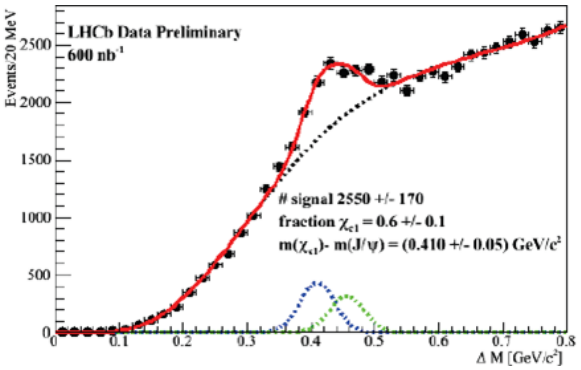

Fig. 10.3 – e^+e^- invariant mass distribution showing a $\chi_{c1,2} \to J/\psi(\mu^+\mu^-)\gamma$ signal.

10.2.1 Tracker Turicensis: operation and performance

The Tracker Turicensis (TT) was constructed at the Physics Institute and has been described in previous annual reports [3]. After its installation in LHCb the detector was operated with high efficiency during the entire data taking period. By the time of the LHC turn on in October 2009 more than 99% of the 144'000 detector channels were fully operational. The average hit detection efficiency was found to exceed 99%. During 2010 some of the readout channels were lost due to broken bond wires. All affected modules have been repaired in Zurich during the Christmas shutdown. S. Saornil and M. Tobin are in charge of maintaining a stable and efficient operation of the TT and monitoring its performance while N. Chiapolini is responsible for its alignment.

10.3 Physics results

10.3.1 J/ψ production and $b\bar{b}$ cross section

Measurements of differential cross sections for prompt J/ψ and $b \to J/\psi X$ production have been performed using 5.2 pb^{-1} of data [29]. The measurement was performed in two-dimensional bins of pseudo-rapidity from $2 < \eta < 4.5$ and transverse momentum from $0 < p_T < 14$ GeV. To separate prompt J/ψ and J/ψ from b decays, the pseudo proper time $t_z = \Delta z \cdot M_{J/\psi}/p_z$ was used, where

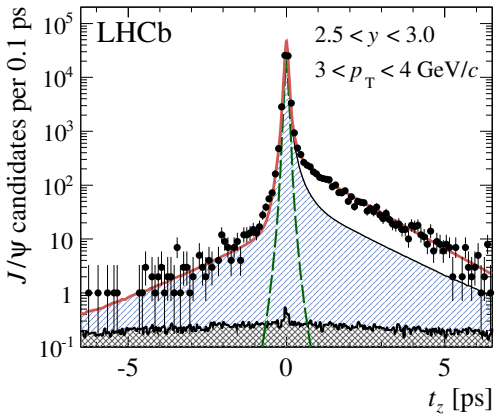

Fig. 10.4 – Distribution of the J/ψ "pseudo proper time" t_z in one of the (p_T, η) bins used in the measurement of differential J/ψ cross sections.

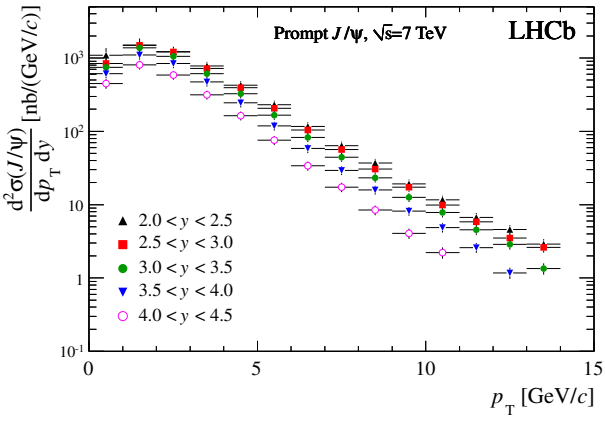

Fig. 10.5 – Prompt J/Ψ production cross-section as a function of p_T in bins of y, assuming no polarisation of the prompt J/ψ.

Δz is the displacement of the J/ψ vertex from the primary vertex along the beam axis, $M_{J/\psi}$ is the J/ψ mass and p_z is the component of the J/ψ momentum along the beam axis. The distribution of t_z in one of the (p_T, η) bins used in the analysis is shown in Fig. 10.4. Combinatorial backgrounds in the t_Z distribution were estimated by combining J/ψ vertices from one event with primary vertices from a different event. The dominating uncertainty on the prompt J/ψ cross section is due to the still unknown J/ψ polarisation in prompt production. Its measurement in LHCb requires a larger data sample. The differential cross section assuming unpolarised J/ψ production is shown in Fig. 10.5. The results are in good general agreement with recent theoretical calculations at high p_T, although the uncertainties on these predictions are still rather large.

The LHCb Monte Carlo simulation, based on PYTHIA 6.4 [30] and EvtGen [31], was used to extrapolate the measured $b \to J/\psi X$ cross section from the LHCb acceptance to the full polar angle range. Using the average $b \to J/\psi X$ branching fraction for inclusive b-hadron decays to J/ψ measured at LEP [32], a $b\bar{b}$ production cross section of $\sigma(pp \to b\bar{b}X) = 288 \pm 4 \pm 48$ μb is calculated. This result is in excellent agreement with an earlier LHCb measurement of the $b\bar{b}$ production cross section that was based on 15 nb^{-1} of data and used $B^0 \to D^0\mu^- X^+$ decays [5]. In this analysis, the impact parameter of the reconstructed D^0 momentum with respect to the primary vertex was used to identify D mesons from b decays and wrong-sign $D^0\mu^+$ combinations were used to estimate backgrounds. Here, a $b\bar{b}$ production cross section of $\sigma(pp \to b\bar{b}X) = 284 \pm 20 \pm 49$ μb was calculated for the full polar angle range, in good agreement with the newer and more precise measurement. Prior to these measurements, simulation studies assessing the LHCb physics reach had assumed a $b\bar{b}$ production cross section of 250 μb at $\sqrt{s} = 7$ TeV.

10.3.2 Direct CP violation in charged charmless B decays

A measurement of direct CP violation in charged charmless hadronic two-body decays is ongoing [13]. Competitive results with previous measurements from the B factories and the Tevatron can be expected from the 2011 data sample. An invariant mass distribution for $B^0_{d,s} \to K^\pm\pi^\mp$ decays was already shown in Fig. 10.2 above. Separating the event sample further into $B^0_d, \bar{B}^0_s \to K^+\pi^-$ and $\bar{B}^0_d, B^0_s \to K^-\pi^+$, a clear difference in event yields is visible in the invariant mass spectra shown in Fig. 10.6. The raw asymmetry between the B^0 and $\bar{B}^0$ yields deviates from zero at the level of three standard deviations and is compatible with

the known world average CP asymmetry. An asymmetry is also visible in the B_s^0 vs. $\bar{B}_s^0$ event yields although the effect is not yet statistically significant, here. The distributions are not corrected for production and detection asymmetries. These corrections, however, are expected to be small.

10.3.3 $B_s^0\,\bar{B}_s^0$ flavour oscillations

The ability to resolve the fast $B_s^0\bar{B}_s^0$ flavour oscillations is an important ingredient for several LHCb key measurements. A measurement of the $B_s^0\bar{B}_s^0$ oscillation frequency in $B_s^0 \to D_s^-(3)\pi$ decay modes has been presented. Despite the still limited statistics, a competitive measurement with existing results from the Tevatron is obtained due to the excellent proper-time resolution of the experiment. Another important ingredient for oscillation measurements is the ability to tag the initial flavour of the B meson at production. Opposite-side lepton, kaon and vertex-charge tags make use of distinctive signatures from the decay of the accompanying b hadron in the event to imply the flavour of the B meson under study. Same-side tags directly determine the flavour of the B meson under study, using the charge of a pion, in the B^0 case, or a kaon, in that of the B_s^0, from the b quark fragmentation chain or from the decay of excited B states. Flavour-specific decay channels such as $B^+ \to J/\psi K^+$, $B^0 \to J/\psi K^\star(K^+\pi^-)$ and $B^0 \to D^0\mu^+\nu_\mu$ are employed to optimise and calibrate the flavour-tagging algorithms. As an example of the tagging performance, Fig. 10.7 shows the observed flavour asymmetry as a function of the B meson proper time for decays $B^0 \to D^0\mu^+\nu_\mu$. The initial flavour at production was determined using opposite side lepton and kaon tags, the flavour at decay is given by the charge of the final state muon. The flavour oscillation is clearly visible and in good agreement with the known $B^0\bar{B}^0$ oscillation frequency Δm_d.

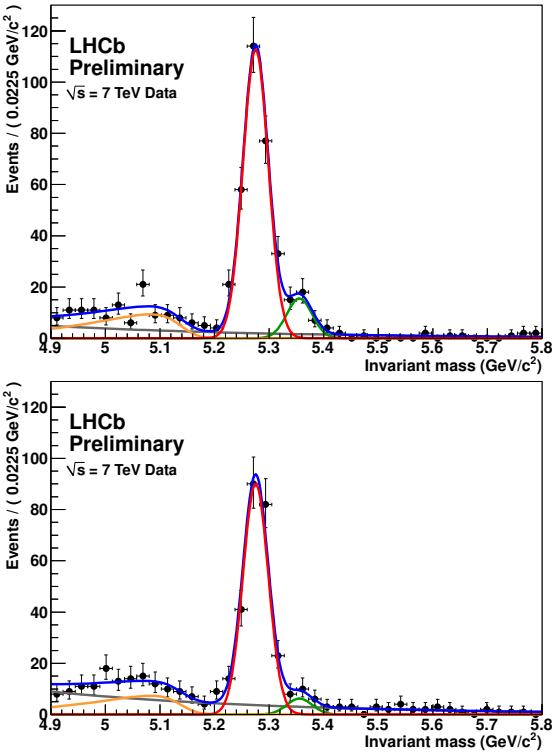

Fig. 10.6 – Invariant mass distributions for $B_d^0\,,\bar{B}_s^0 \to K^+\pi^-$ (top) and $\bar{B}_d^0\,,B_s^0 \to K^-\pi^+$ (bottom). Red: fitted signals from B_d^0 and $\bar{B}_d^0$ decays; green: B_s^0 and $\bar{B}_s^0$ decays; yellow: background from mis-identified three-body decays; grey: combinatorial background. No corrections were made for production- and detector asymmetries.

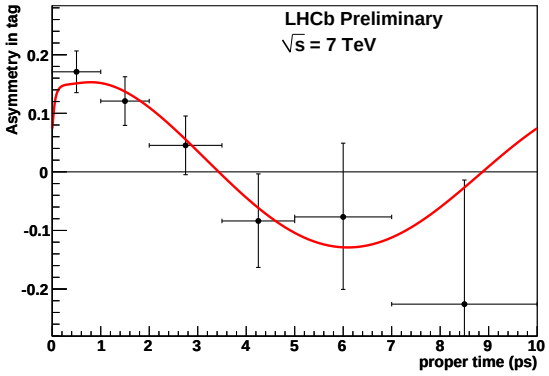

Fig. 10.7 – Flavour asymmetry as a function of the B proper time in $B \to D\mu\nu_\mu$ decays. Opposite-side lepton and kaon taggers were used to tag the initial flavour of the B meson. The overlayed fit function was obtained fixing Δm_d to its PDG value [38].

10.3.4 The rare decay $B_s \to \mu\mu$

A. Büchler, Ch. Elsasser, J. van Tilburg, N. Serra and O. Steinkamp are deeply involved in this key LHCb measurement. The present best upper limits on the branching fraction, reported by the Tevatron experiments [34; 35], are still an order of magnitude above the SM prediction $(3.35 \pm 0.32) \times 10^{-9}$ [33] leaving room for a clear NP signal. On the other hand, reducing the current limits would severely constrain the parameter space for NP models [36]. An upper limit close to the best limits reported by the Tevatron experiments is obtained already from the relatively small data set. This first LHCb result has been shown at conferences and is accepted for publication [37]. For 1 fb^{-1} collected in 2011, a 90% exclusion limit approaching the SM branching fraction is expected if no signal is observed. A 5σ observation of the SM value will require 6-10 fb^{-1}. The analysis strategy is described in detail in Ref. [2]. An important feature is the extensive use of control channels in order to reduce the dependency on simulation. Here, the analysis profits from the large samples of hadronic two-body B decays that LHCb collects.

One of the fields of activity of our group is the calibration of the invariant mass likelihood. The $\mu^+\mu^-$ invariant mass is the main variable distinguishing signal from background. The invariant mass resolution for B_s was studied by Ch. Elsasser by interpolating the resolution for the resonances J/Ψ, $\Psi(2S)$, $\Upsilon(1S)$, $\Upsilon(2S)$ and $\Upsilon(3S)$. The result was found in good agreement with the invariant mass resolution extracted from $B \to hh$ decays.

An alternative method which is expected to reduce the background is studied by A. Büchler. In her thesis she determines an event-by-event invariant mass error for each $\mu^+\mu^-$ candidate by propagating the errors on the muon momenta and the opening angle between the two muons obtained from the track and vertex fit. The method corrects for biases in the errors given by the track and the vertex. It is calibrated and tested using other two-body decays such as $J/\Psi \to \mu^+\mu^-$, $J/\Psi \to \mu^+\mu^-$ and $B \to hh$. At hadron colliders the luminosity and the production cross section are generally poorly known so it is more convenient to do relative measurements. There are several well known $B_{d,u}$ branching ratios measured by B-factories which can be used. In particular the $B^+ \to J/\Psi K^+$ branching ratio is known at 3% level. This mode has a similar trigger and the same particle identification as the $B_s \to \mu^+\mu^-$ decay. The dominant uncertainty with this strategy will be the ratio of fragmentation fractions $f_s/f_{d,u}$, which was measured to about 12% precision at LEP [39].

A method for determining f_s/f_d in a model independent way using the relative yields of $B^0_{d,s} \to D^-_{d,s}\pi^+$ and $B^0_{d,s} \to D^-_{d,s}K^+$ measured by LHCb has been proposed [40]. A precision of 6-9% on f_s/f_d from this analysis is expected by summer 2011. Preliminary results with a precision close to the world best were presented at winter conferences [12].

10.3.5 Lepton Flavour Violating B-decays

Given the large number of B-mesons, the high momentum resolution and efficient particle identification, LHCb has the potential to greatly improve the sensitivity to Lepton Flavour Violating B-meson decays, e.g. $B_s \to e^\pm\mu^\mp$ and $B_s \to \mu^\pm\tau^\mp$. These decays are forbidden in the SM but they are allowed in several of its extensions, the simplest of these being the Pati-Salam model [41], where a leptoquark exchange can mediate these decays at tree level.

Here we can profit of our groups experience in rare decays, in particular $B_s \to \mu^+\mu^-$. Ch. Elsasser, collaborating with N. Serra and O. Steinkamp, will focus on the study of these decay channels using 2011-2012 data.

10.3.6 $B^0 \to K^\star\mu^+\mu^-$

Angular distributions in the rare decay $B^0 \to K^\star\mu^+\mu^-$ give rise to several observables that are sensitive to NP contributions [42]. Very promising is the forward-backward asymmetry A_{FB}, defined by the angle between the μ^- direction and the direction of the B^0 measured in the rest frame of the $\mu^+\mu^-$ system. First measurements of A_{FB} as a

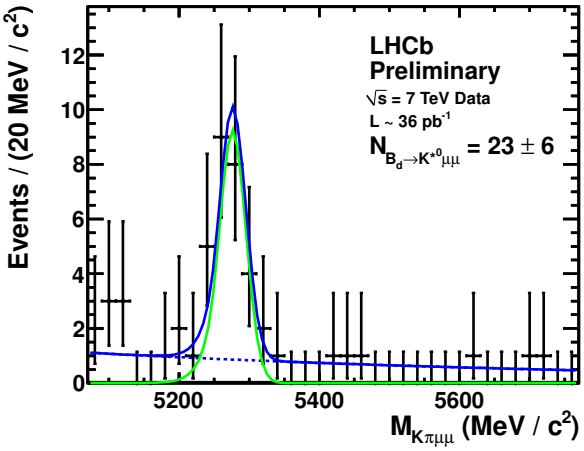

Fig. 10.8 – $K\pi\mu\mu$ invariant mass distribution showing a clear $B^0 \to K^\star\mu^+\mu^-$ signal.

function of the dilepton invariant mass squared q^2 have been published by the BaBar [43], Belle [44] and CDF [45] collaborations. All three experiments observed a flipped sign of A_{FB} in the low q^2 region, larger than predicted by the SM although the statistical precision is still too low for definitive conclusions.

Already with the 37 pb^{-1} of data accumulated in 2010, LHCb observes a clear $B^0 \to K^\star\mu^+\mu^-$ signal, as shown in Fig 10.8. With only 100 pb^{-1} of data, LHCb will reach a sensitivity to A_{FB} that is similar to the current measurements from the B factories and CDF. Assuming the same central value as measured by Belle, a 5 σ deviation from the SM could be measured by LHCb with about 1 fb^{-1} of data.

One of the most critical aspects of the analysis are possible biases on the angular distributions due to detector acceptance and selection cuts. J. Anderson, M. De Cian, Ch. Salzmann and N. Serra play a key role in this aspect of the analysis. Given the good agreement between measurement and simulation demonstrated with 2010 data we intend to make event-by-event corrections based on the simulation. The procedure will be validated on the control channel $B^0 \to J/\Psi(\mu^+\mu^-)K^\star$ which has the same final state as the $B^0 \to K^\star\mu^+\mu^-$ but about 50 times more statistics. A similar strategy will be used to evaluate systematics uncertainties. Ch. Salzmann has shown how this validation can be performed using $B^0 \to J/\Psi K^*$ data collected in 2010. The correction uses several inputs such as the particle identification efficiencies. M. De Cian is studying how to extract these efficiencies from the measurement using a tag and probe method.

10.3.7 Forward electroweak physics

J. Anderson, A. Bursche, N. Chiapolini, and K. Müller are involved in measurements of W, Z and Drell-Yan production in the forward region which provide an important test of the SM. Theoretical predictions are known to next-to-next-to leading order in perturbative QCD [46] and the uncertainties vary between 3% and 10% depending on rapidity, where the dominant uncertainty is due to the knowledge of the parton distribution functions (PDFs) of the proton. Measurements of the differential cross sections for electroweak bosons decaying into muon final states and the ratios of these cross sections can probe the parton density functions at low x where the PDFs are hardly constrained by previous measurements and also test the QCD predictions in a previously unexplored region. Preliminary results on differential cross section measurements and ratios of W and Z production based on 16.5 pb^{-1} have been presented at several conferences [19].

The results are summarised in Fig. 10.9 for final state muons having transverse momenta larger

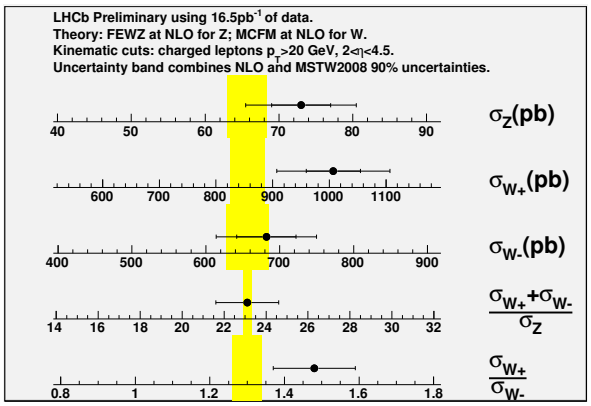

Fig. 10.9 – Summary of W and Z production cross sections and cross section ratios with muons in the pseudo-rapidity range $2 < \eta_\mu < 4.5$ and transverse momentum larger than 20 GeV. The vertical band indicates the theory prediction with its error.

than 20 GeV and lying within pseudorapidities $2 < \eta_\mu < 4.5$. In addition, the invariant mass of the two muons from the Z boson decay must be between $81 < m_Z < 101$ GeV. All cross sections and ratios are in good agreement with next-to-leading order predictions [47]. The precision will significantly improve with a more precise determination of the luminosity. The cross section ratios which are independent of the luminosity and where some of the systematic errors cancel will constitute a very precise test of the SM with increased statistics. Already by the end of 2011 all these measurements will be limited by systematics.

A key ingredient is the determination of various efficiencies from the measured data. Here, our group is making significant contributions. A. Bursche has developed techniques to monitor the trigger efficiency for W and Z which both require one muon with high transverse momentum in the trigger and also for Drell-Yan events which are triggered by the di-muon trigger. The offline tracking efficiency was determined by M. De Cian using a tag and probe method. The same method is used to measure the tracking efficiency in J/Ψ or Υ decays. A tag and probe method is also used by J. Anderson to determine the muon reconstruction efficiency.

In future it is planned to study in more detail the backgrounds for the W analysis and to extend the measurements to events with jets accompanying the electroweak boson (A. Bursche). A detailed understanding of the dominant background (kaons or pions and muons from semileptonic decays) is crucial for the reduction of the systematic error. A measurement of the cross section for jets plus an electroweak boson will be sensitive to the gluon content in the proton. Low mass Drell-Yan will allow to probe PDFs down to Bjorken-x values as low as 10^{-5}. Here, the PDFs are basically not constrained by previous experiments. N. Chiapolini will study Drell-Yan production.

10.4 Summary and outlook

The LHCb experiment has performed very well throughout the 2010 LHC run. About 37 pb^{-1} of data have been recorded, with a data taking efficiency exceeding 90%. A number of early analyses have demonstrated the ability of the LHCb detector to produce high quality results under harsher conditions than the experiment was designed for. Key performance parameters match or are close to expectations from simulation studies. Further improvements are still expected from better calibration and alignment. In addition to what has been discussed in this report, LHCb has already made some world best and world first measurements of B-hadron branching ratios. In several key analyses, sensitivities approaching those of existing measurements can already be expected from the 2010 data sample. With the much larger data sample expected for 2011, LHCb will be able to probe for New Physics signatures.

[1] A.A. Alves Jr. *et al.* [LHCb collaboration], JINST 3 S08005 (2008).

[2] B. Adeva *et al.* [LHCb Collaboration], *Roadmap for selected key measurements of LHCb*, arxiv:0912.4179v2 [hep-ex].

[3] Physik-Institut, University of Zürich, Annual Reports 1996/7 ff.; available at *http://www.physik.unizh.ch/reports.html.*

[4] R. Aaij *et al.* [LHCb Collaboration], Phys. Lett. B**698** (2011) 14-20.

[5] R. Aaij *et al.* [LHCb Collaboration], Phys. Lett. B**694** (2010) 209-216.

[6] Raij *et al.* [LHCb Collaboration], Phys. Lett. B**693** (2010) 69-80.

[7] Preliminary LHCb results presented at 46th Rencontres de Moriond on Electroweak Interactions and Unified Theories, 13 - 20 Mar 2011, La Thuile, Italy, Les Rencontres de Physique de la Vallée d'Aoste, 27 Feb - 5 Mar 2011, La Thuile, Italy, Workshop on Discovery Physics at the LHC, 5 - 10 Dec 2010, Mpumalanga, South Africa, 35th Inter-

national Conference on High Energy Physics, 22 - 28 Jul 2010, Paris, France.

[8] *First observation of the decay* $B_s^0 \to K^{\star 0}\bar{K}^{\star 0}$
CERN-LHCb-CONF-2011-019.

[9] *A measurement of the relative cross-section* $\sigma(X_{c2})/\sigma(X_{c1})$ *prompt* X_c *production at* $\sqrt{s}$ *= 7 TeV in LHCb*
CERN-LHCb-CONF-2011-020.

[10] *Measurement of the* B_c^+ *to* B^+ *production cross-section ratios at* $\sqrt{s}$ *= 7 TeV in LHCb*
CERN-LHCb-CONF-2011-017.

[11] *Inclusive jets and dijets in LHCb*
CERN-LHCb-CONF-2011-015.

[12] *Measurement of the relative yields of the decay modes* $B^0 \to D\pi^+, B^0 \to DK^+, B_s^0 \to D_s^-\pi^+$*, and determination of* fs/fd *for 7 TeV pp collisions*
CERN-LHCb-CONF-2011-013.

[13] *Measurement of direct CP violation in charmless charged two-body B decays at LHCb*
CERN-LHCb-CONF-2011-011.

[14] *Measurement of* Δm_d *in* $B^0 \to D\pi^+$
CERN-LHCb-CONF-2011-010.

[15] *Observation of double* J/Ψ *production in proton-proton collisions at a centre-of-mass energy of* $\sqrt{s}$ *= 7 TeV*
CERN-LHCb-CONF-2011-009.

[16] *First observation of the decay* $\overline{B}_s^0 \to D^0 K^{\star 0}$ *and measurement of the ratio of branching fractions* $\frac{B(\overline{B} \to D^0 K^{\star 0})}{B(\overline{B}_d^0 \to D^0 \rho^0)}$
CERN-LHCb-CONF-2011-008.

[17] *Improved Measurements of the Cabibbo Favored Decays* $B_{(s)} \to D_{(s)}\pi\pi\pi$ *and* $\Lambda_b \to \Lambda_c\pi\pi\pi$ *Branching Fractions*
CERN-LHCb-CONF-2011-007.

[18] *Measurement of* Δm_s *in the decay* $B_s^0 \to D_s(K^+K\pi)(3)\pi$
CERN-LHCb-CONF-2011-005.

[19] *W and Z production at* $\sqrt{s}$*= 7 TeV with the LHCb experiment*
CERN-LHCb-CONF-2011-012.

[20] *Optimization and calibration of the LHCb flavour tagging performance using 2010 data*
CERN-LHCb-CONF-2011-003.

[21] *b-hadron lifetime measurements with exclusive* $b \to J/\Psi X$ *decays reconstructed in the 2010 data*
CERN-LHCb-CONF-2011-001.

[22] *Measurement of the inclusive* Φ *cross-section in pp collisions at* $\sqrt{s}$*=7TeV with the LHCb experiment*
CERN-LHCb-CONF-2010-014.

[23] *Prompt charm production in pp collisions at s = 7 TeV*
CERN-LHCb-CONF-2010-013.

[24] *Measurements of* B^0 *mesons production cross-section in pp collisions at* $\sqrt{s} = 7$ *TeV using* $B^0 \to D^{\star -}\mu^+\nu_\mu X$ *decays*
CERN-LHCb-CONF-2010-012.

[25] *Measurement of prompt* $\overline{\Lambda}/\Lambda$ *and* $\overline{\Lambda}/K_S^0$ *production ratios in inelastic non-diffractive pp collisions at s = 0.9 and 7 TeV*
CERN-LHCb-CONF-2010-011.

[26] *Measurement of the* J/Ψ *production cross-section at* $\sqrt{s}$ *= 7 TeV in LHCb*
CERN-LHCb-CONF-2010-010.

[27] *Measurement of the* $\overline{p}/p$ *ratio in LHCb at* $\sqrt{s}$ *= 900 GeV and 7 TeV*
CERN-LHCb-CONF-2010-009.

[28] *Prompt* K_S^0 *production in pp collisions at* $\sqrt{s}$ *= 900 GeV*
CERN-LHCb-CONF-2010-008.

[29] R. Aaij *et al.* [LHCb Collaboration], *Measurement of* J/Ψ *production in pp collisions at* $\sqrt{s}$ *= 7 TeV*, submitted to Eur. Phys. J. C, arXiv:1103.0423 [hep-ex].

[30] T. Sjöstrand, S. Mrenna and P.Z. Skands, J. High Energy Phys.**0605** (2006) 026.

[31] D.J. Lange, Nucl. Instrum. and Meth. A**462** (2001) 152.

[32] P. Abreu *et al.* [DELPHI Collaboration], Phys. Lett. B**341** (1994) 109; O. Adriani *et al.* [L3 Collaboration], Phys. Lett. B**317** (1993) 467; D. Buskulic *et al.* [ALEPH Collaboration], Phys. Lett. B**295** (1992) 396.

[33] M. Blanke, A. Buras, D. Guadagnoli and C. Tarantino, JHEP 0610:003 (2006).

[34] V. Abazov *et al.* [D0 Collaboration], Phys. Lett. B**693** (2010) 539.

[35] CDF preliminary, *Search for* $B_s^0 \to \mu^+\mu^-$ *and* $B_d^0 \to \mu^+\mu^-$ *Decays in 3.7* fb^{-1} *of* $p\bar{p}$ *Collisions with CDFII*, CDF Public Note 9892.

[36] O. Buchmüller *et al.*,
Eur. Phys. J. C**64** (2009) 391.

[37] R. Aaij *et al.* [LHCb Collaboration],
Search for the rare decays $B_s^0 \to \mu^+\mu^-$ *and* $B^0 \to \mu^+\mu^-$, accepted by Phys. Lett. B, arxiv:1103.2465v1 [hep-ex].

[38] K. Nakamura *et al.* [Particle Data Group],
J. Phys. G **37** (2010) 075021.

[39] D. Asner *et al.*,
Averages of b-hadron, c-hadron, and tau-lepton Properties, arXiv:1010.1589,

[40] R. Fleischer, N. Serra and N. Tuning,
Phys. Rev. D**82** (2010) 034038.

[41] J. Pati and A. Salam, Phys. Rev. D**10** (1974), 275.

[42] J. Altmannshofer *et al.*,
JHEP **0901** (2009) 019;
F. Kruger and J. Matias,
Phys. Rev. D**71** (2005) 094009;
U. Egede *et al.*, JHEP**032** (2008) 0811.

[43] B. Aubert *et al.*,
Phys. Rev. D**79** (2009) 031102.

[44] J.T. Wei *et al.*,
Phys. Rev. Lett.**103** (2009) 171801.

[45] T. Aaltonen *et al.*,
Phys. Rev. D **79** (2009) 011104.

[46] R. Gavin *et al.*, arXiv:1011.3540 [hep-ph].

[47] J. M. Campbell, R. K. Ellis,
Phys. Rev. D**62** (2000) 114012.